This is the author's version (manuscript) of the work that was accepted for publication in Mechanics of Advanced Materials and Structures.
The Version of Record is available online at 10.1080/15376494.2022.2132436

Novel approach combining two homogenization procedures for the analysis of nonwoven biocomposites

X. Martinez[a,b,*], J. Bachmann[c], F. Otero[a,b], S. Oller[a], G. Bugeda[a,d]

a. International Center for Numerical Methods in Engineering (CIMNE). Campus Nord, Gran Capità s/n, 08034 Barcelona, Spain

b. Department of Nautical Science and Engineering - Universitat Politècnica de Catalunya (UPC). Pla de Palau 18, 08003 Barcelona, Spain

c. DLR – Deutsches Zentrum für Luft- und Raumfahrt e.V. (German Aerospace Centre), Institute of Composite Structures and Adaptive Systems, Braunschweig, Germany

d. Department of Civil and Environmental Engineering – Universitat Politècnica de Catalunya (UPC). Campus Nord, Gran Capità s/n, 08034 Barcelona, Spain

Key words: Natural fibre composites (NFC), Nonwoven, Three-point bending test (3PB), Multiscale modelling, Equivalent Representative Volume Element (ERVE)

Abstract.

Composite materials with complex internal microstructures, such as the flax nonwoven bio-composite studied in this work, require advanced numerical models in order to predict their mechanical performance. Otherwise, the micro-structural interactions that take place between their components makes very difficult to obtain their mechanical properties and failure mechanisms. This paper presents a novel methodology that couples two homogenization formulations: a phenomenological one, the serial-parallel mixing theory; and a numerical multiscale procedure. The resulting methodology has a minimal computational cost, while it is capable to account for the different interactions that take place among the composite constituents. With the proposed approach, it is possible to characterize the mechanical response of nonwoven composites and to predict their structural failure. The methodology developed is applied to a flax nonwoven bio-composite manufactured and tested by the German Aerospace Center (DLR). The good results obtained from the simulation, when compared with the experimental values, allow considering the proposed procedure an excellent approach for the analysis of large structures made with complex microstructures, such as nonwoven biocomposites.

* Corresponding author: x.martinez@upc.edu

1 INTRODUCTION

The environmental advantages in weight reduction that have been accomplished by using composite materials in engineering structures, from planes to ships or cars, can be overshadowed by the difficulties that these materials have for their disposal and recyclability, and by the large quantity of material that will reach its end of life (EoL) in the following years. Based on the study made by Lefeubre *et al.* [1], in 2050 the commercial aeronautical sector will have generated about 527,374 tons of CFRP waste globally, if nothing has been done to recycle it before then. Being aware of this problem, many efforts are set to find efficient procedures to recycle oil-based composites. Most of them are described in the review made by Karuppannan and Kärki in [2]. In their study these authors show that although recyclable procedures are improving, they are still far from being commercially profitable and completely efficient. In this scenario, the use of bio-based composite materials is an excellent alternative to reduce the environmental footprint of low-weight materials.

Bio-based composites are obtained by mixing natural fibres in a matrix system, which can be also bio-based. The interest on these materials have provided a large number of bio-materials that can be used as fibres, from wood [3], to hemp [4] or flax [5]. Although the mechanical performance of these materials is lower than the one that can be obtained with Carbon Fiber Reinforced Polymers (CFRP) or Glass Fiber Reinforced Polymers (GFRP), it is sufficient for the requirements of many industries and applications, as it is shown in the review made by Mohammed et al. in [6], or as it has been proved in the EU funded project Eco-Compass [7], [8]. However, in order for eco-composites to be a real alternative to synthetic composites, it is necessary to improve the existing knowledge about them, as well as to have analysis and simulation tools capable of representing their performance accurately. This will ensure that the new structures designed with eco-composites comply with the required security, functionality and quality standards.

There are many challenges to overcome in order to predict accurately the mechanical performance of natural fibre composites (NFCs), and this may be the reason why most of the work conducted to characterize their behaviour is based on experimental measurements. Some of these challenges are the dispersion in the fibre properties [9], [10], the effect of fibre waviness in the composite response

[11], [12], or the fact that most of the composites use relatively short fibres, between 10 and 100mm, to produce nonwoven composites. This last challenge is pointed out in the review made by Mohammed et al. [6] in which the authors state that most of the applications use NCF in a mat, or nonwoven, from.

Nonwoven composites are made with relatively short fibres, which commonly present large waviness, a wide distribution of fibre cross section, and a random orientation. Their complex microstructure makes their geometric characterization very difficult, making necessary the use of advanced techniques to obtain an exact reconstruction of their internal microstructure [13]. For this reason, most of the formulations developed to characterize these materials are based on analytical models, such as the one proposed by Qiu and Fan [14] which is based on the Ramberg-Osgood equations, or the model developed by Zhang *et al.* [15] which is based on the analytical response of a single fibre, either curved or straight. This last model is validated with the results obtained from a Representative Volume Element (RVE) of the nonwoven composite.

The use of the Finite Element Method (FEM), together with multiscale strategies based on the analysis of RVEs, is becoming common to study the mechanical performance of composites with complex microstructures. However, the computational cost of these methods forces to make large simplifications in order to conduct the analysis, such as in the approach followed by Farukh et al. [16], [17] to study nonwovens. In this work fibres have been considered straight and have been modelled with beam elements. In other cases, the analysis is limited to the prediction of the mechanical properties, linear and non-linear, provided by the RVE. This is is done in the work of Naili *et al.* [18] for short fibre reinforced composites, and in the work by Greco *et al.* [19] in which it is evaluated the non-linear effect produced by different micro-cracks configurations in a UD composite. To other works worth mentioning that use RVE analyses to obtain the non-linear performance of the material, are the ones of Levrero-Florencio *et al.* [20], [21] and Werner *et al.* [22], these authors use the RVE to characterize the non-linear performance of trabecular bone. In these studies the authors use a RVE obtained from a micro CT scan that does not fulfil the periodicity condition usually required in multiscale procedures.

Current work presents a novel approach that combines two homogenization procedures for the analysis of nonwoven biocomposites. One of the procedures is a phenomenological homogenization, the serial-parallel mixing theory (SP RoM) [23], which obtains the performance of the composite by means of the mechanical response of its constituents. This formulation is very efficient computationally and allows solving large structures and predicting their failure mechanism taking into account most composite micro-structural characteristics [24], [25]. The material parameters defined in this first homogenization procedure will be modified based on the results obtained from a multiscale numerical homogenization [26], in order to take into account some composite properties that cannot be taken into account by the SP RoM, such as fibre waviness. The use of a multiscale numerical homogenization to characterize a nonwoven composite requires reformulating the concept of RVE to what will be called Equivalent Representative Volume Element (ERVE), as now the material does not present a periodic microstructure that fulfils the scale separation condition [27], [28]. A similar approach has been already followed by some authors, such as the abovementioned Levrero-Florencio et al. [20], [21] and Werner et al. [22], as their micro-RVE does not fulfil the periodicity condition either.

In the following are presented the formulations that will be used in this work. Afterwards it is described the flax nonwoven biocomposite manufactured and tested. This material is used afterwards to describe and exemplify the procedure developed for the analysis of nonwoven composites. Finally, the procedure is validated with the analysis of a 4PB test of the material.

2 HOMOGENIZATION PROCEDURES FOR THE ANALYSIS OF COMPOSITE MATERIALS

A homogenization procedure consists on obtaining the material properties (homogenized properties) from a model that accounts for the internal structure of the material. This model can be either numerical or analytical.

Traditionally, composites have been characterized as orthotropic elastic materials, coupled with specific formulations that provide their failure onset based on specific failure criteria. Examples of such approaches can be found in [29]. These formulations are a basic form of a homogenization procedure, as they provide an average characterization of the composite performance. However, the simplicity of these formulations makes necessary a detailed calibration process for each composite material analysed, and limits the amount of information provided by the model, as they do not have any information about the interaction between the composite constituents.

In order to obtain a more detailed description of the composite performance, it is necessary to use more complex formulations that must account for the response of the composite constituent materials and their possible interactions. Following this approach, this work uses two different ones: the Serial-Parallel mixing theory (SP RoM) [23] and a multiscale computational homogenization [26]. The first one couples the performance of the composite constituents by defining a set of compatibility equations between their constitutive laws; while the second one obtains the response of the composite from a numerical model representing the microstructure of the material. These two formulations are described in the following. As both formulations rely on the constitutive performance of the composite components, this section also includes a brief description of the damage law used by the models, as well as a mapping space anisotropy procedure used to improve the accuracy of the constitutive laws used.

2.1 Serial-parallel mixing theory

The mixing theory was initially proposed by Truesdell and Toupin [30] as a set of hypothesis for coupling the response of materials made with different constituents. In its original form, the main assumptions of the theory are that all materials contribute to the global response proportionally to their volumetric participation, and that they all share the same strain field. Following a similar approach, the inverse mixing theory is formulated imposing that all materials share the same stress field.

Several authors have used the initial hypothesis defined by Truesdell and Toupin to provide new models to characterize composite materials. Among them it is worth to mention the efforts made by Sergio Oller and co-authors, who have transformed the original mixing theory into a constitutive equation manager, capable of providing the mechanical response of the composite from the constitutive performance of its constituents, in the linear and non-linear range. The different developments conducted in this field are described in [31], [32]. Departing from this initial research, Rastellini *et al.* [23] proposed the so called Serial-parallel mixing theory, which is one of the formulations that will be used in current work. The basics of this formulation are described hereafter.

The serial-parallel mixing theory is based on five different hypotheses:

1. The constituent materials of the composite are subjected to the same strain in the parallel direction. Usually this direction corresponds to the fibre orientation.
2. The constituent materials are subjected to the same stress in the serial direction.
3. The response of the composite material is directly related to the volume fractions of its constituent materials.
4. The phases in the composite are considered to be homogeneously distributed.
5. The constituent materials are considered to be perfectly bonded.

Of these hypotheses, the first two are the closing equations that provide the relation between the composite components. If these conditions are applied to a two-component composite, consisting of fibres embedded in a matrix, these equations can be written as:

$$\begin{aligned} &\text{Parallel behaviour:} \quad \begin{cases} {}^{c}\varepsilon_P = {}^{m}\varepsilon_P = {}^{f}\varepsilon_P \\ {}^{c}\sigma_P = {}^{m}k\ {}^{m}\sigma_P + {}^{f}k\ {}^{f}\sigma_P \end{cases} \\ &\text{Serial behaviour:} \quad \begin{cases} {}^{c}\varepsilon_S = {}^{m}k\ {}^{m}\varepsilon_S + {}^{f}k\ {}^{f}\varepsilon_S \\ {}^{c}\sigma_S = {}^{m}\sigma_S = {}^{f}\sigma_S \end{cases} \end{aligned} \tag{1}$$

Where c, m and f state for composite, matrix and fibre, P and S correspond to the parallel and serial direction, and ${}^{i}k$ is the volumetric participation of the component in the composite.

The implementation of the serial-parallel mixing theory in a Finite Element code is explained in detail in ([23], [33]). It is based in an initial prediction of the composite constituent strains, assuming that they have a linear-elastic behaviour. Once knowing the strain tensor of fibre and matrix, it is possible to apply the constitutive model to each material to obtain their respective stress tensor, which must fulfil the iso-stress condition in the serial direction. If the materials have not reached their failure threshold stress, the elastic prediction made is correct and the iso-stress condition is fulfilled.

Otherwise, the initial prediction does not lead to an iso-stress condition, and it is necessary to start an iterative procedure until reaching a strain-stress state for both components that verifies the closing equation.

The capabilities of the formulation to predict the mechanical performance of composite laminates in the linear and non-linear range, as well as the procedure required to obtain the material parameters from experimental tests, is described in [34]. There are several studies that show the capabilities of the formulation to predict different composite failures, such as delamination [24], [35], delamination due to compression [25] or open-hole failure compression [36].

2.2 Numerical multiscale procedure

A numerical multiscale procedure deals with the analysis of the composite structure in a two-scale context. In the first scale, named macroscale, the model obtains the global response of the structure. In this scale composites are treated as homogeneous materials. The second scale, named microscopic or local scale, characterizes an elemental characteristic volume in which the microscopic fields inside the composite are obtained.

The basic principles of homogenization method were defined by Suquet [37] in order to obtain the constitutive equation for homogenized properties of a heterogeneous material. The unit cell is defined as a microscopic sub-region that is representative of the entire microstructure in an average sense. The Representative Volume Element (RVE) is employed to obtain the effective properties for the homogenized material because it is assumed that it must contain a sufficient number of heterogeneities [27], [38]. The first-order homogenization framework used in this work takes knowledge from the theory proposed by Zalamea and Oller [39], and by Badillo and Oller [40]. Their developments where further improved and extended to a tri-dimensional framework by Otero *et al.* in [26]. The homogenization technique described in [26] assumes that there is a scale separation between the macro and the microstructures, which means that the characteristic length of the microscale l must be much smaller than the length of the macroscale elements, L: $l \ll L$ [27], [28].

Another basic assumption made by the theory is the periodicity of the representative volume element in the material microstructure [39].

The solution of the problem at the microscale acts as an equivalent constitutive law for the macroscale, and it provides material stiffness and stresses from the volume average of the microscopic ones. This equivalent constitutive law is used in all the integration points of the macro-model in order to obtain the response of the structure. In case of having a non-linear behaviour of the microscopic model, it will lead to an iterative procedure in which the RVE must be solved for different boundary conditions until both scales reach equilibrium, ensuring consistency between the micro- and macroscale solutions. A schematic representation of a homogenization method is shown in Figure 1. With this approach, complex finite element models can be used to simulate the composite microstructure, taking into account microstructural phenomena such as fibre-matrix debonding, matrix degradation, thermal effects, performance of woven-type composites, etc.

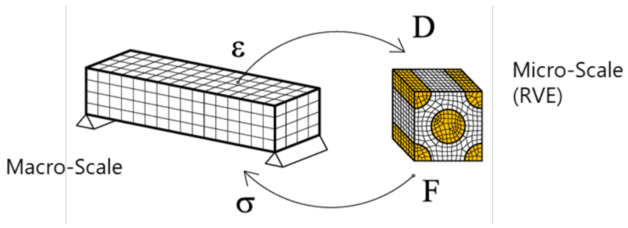

Figure 1. Schematic representation of a multiscale analysis. Strains (ε) in the macro-model are transformed to displacements (D) in the micro-model, and the resultant forces (F) in the micro-model are transformed to stresses (σ) in the macro-model

One of the major drawbacks of numerical multiscale procedures is their computational cost, especially when the macro and the microstructures are defined with many details. This problem is highlighted in the work by Otero et al. [41], in which the cost of the numerical multiscale method was compared with the cost of the SP RoM. To overcome this drawback, several strategies have been proposed to minimize the computational cost [42], [43], although they are still expensive and cannot be used as a common procedure yet.

2.2.1 Macro to micro transition

The mathematical foundations of a multiscale analysis and its numerical implementation are fully described in the work of Otero *et al.* [26]. The basic principle used to transfer information between both scales is through the definition of a micro-mechanical displacement on the RVE associated to the existing displacements in the macroscale:

$$u_\mu = u + w(X_\mu) \tag{2}$$

being , u and u_μ the displacements at the macroscale and the microscale, respectively. And $w(X_\mu)$ the micro-fluctuations on the RVE, which vary for each point in the microscale X_μ.

The relation between both scales is made through the averaging theorems [44], these state that the effect of the microscale over the macroscale can be obtained as the integral over a representative volume element. If this is applied to obtain the deformation gradient, F, it can be written:

$$F(X_0) = \frac{1}{V_\mu}\int_{V_\mu} F_\mu(X_0, X_\mu)\, dV \tag{3}$$

where $F(X_0)$ is the deformation gradient of the macro-structure in the considered point X_0, V_μ is the RVE volume, and F_μ are the deformation gradients at the different points of the RVE. Using this last expression together with the microscale displacements defined in equation (3), it is possible to obtain different sets of boundary conditions that relate the displacements of the macro- and micro-models. These are the following:

i. Taylor model (or zero fluctuations): $w(X_\mu) = 0 \quad \forall X_\mu \in V_\mu$

   This model gives homogeneous deformation in the microstructural scale level. The results provided by this model are equivalent to those provided by the mixing theory.

ii. Linear boundary displacements (or zero boundary fluctuations): $w(X_\mu) = 0 \;\; \forall X_\mu \in \partial V_\mu$.

   Being ∂V_μ the boundary of the RVE. In this case, the deformation of the RVE boundary domain is fully prescribed.

iii. Periodic boundary fluctuations: $w(X_\mu^+) = w(X_\mu^-) \;\; \forall\, X_\mu \in \{\partial V_\mu^+, \partial V_\mu^-\}$.

   In this case, the kinematical constraint defines a periodic displacement fluctuation on the different faces of the RVE.

iv. Minimal constraint (or uniform boundary traction): This case obtains the nontrivial solution of $\int_{\partial V_\mu} w \otimes_s N dA = 0$. In this expression N corresponds to the normal to the undeformed boundary of the RVE.

Among these four possibilities, the one most commonly used is the periodic boundary condition, because it generally provides an intermediate and more exact response compared to other type of boundary conditions, as it is described in [26], [38].

2.2.2 Micro to macro transition

Once the boundary conditions that must be applied to the micro-model to characterize the material performance are known, it is possible to solve the Boundary Value Problem (BVP) and to obtain the stress state of the different elements in which the RVE is discretized. The homogenized stress tensor in the macroscale is obtained by means of the average theorem, as:

$$\sigma(X_0) = \frac{1}{V_\mu} \int_{\mathrm{V}_\mu} \sigma_\mu(X_0, X_\mu) dV \tag{4}$$

2.2.3 Equivalent Representative Volume Element (ERVE)

One of the main assumptions made by multiscale procedures to define a Representative Volume Element (RVE) is that the microstructure of the material is periodic, and that this periodicity is represented in the RVE defined [27], [35]. This assumption cannot be applied to simulate materials with a non-periodic microstructure, such as the nonwoven eco-composites considered in this work, because the periodicity is inexistent in the material due to the randomness of the fibre configuration.

This work modifies the concept of RVE to define what will be called an Equivalent Representative Volume Element (ERVE). An ERVE is defined as a periodic micro-model that is capable to capture the mechanical response of the material, with no further requirements or constrains. Therefore, it is possible that the microstructure defined in the micromodel do not exist in the real material or, if it exists, it may not be periodically repeated. However, the response obtained from the ERVE must be similar to the one produced by the real material. An ERVE can be understood as a mathematical model (based on a numerical analysis) that provides the material response, as it is done by constitutive equations, but that does not replicate the exact material geometry and configuration. Figure 2 shows the implications of using a micro-model as an RVE or as an ERVE. In the first case, the micro-model is biunivocally related to a periodic material, while in the second case the requirement of the micro-model is to be able to represent the material performance, but it does not have to correspond to a specific pattern in the material.

The ERVE is defined with a geometrical periodicity in its boundaries. This is required in order to be able to use the multiscale formulation described in this section.

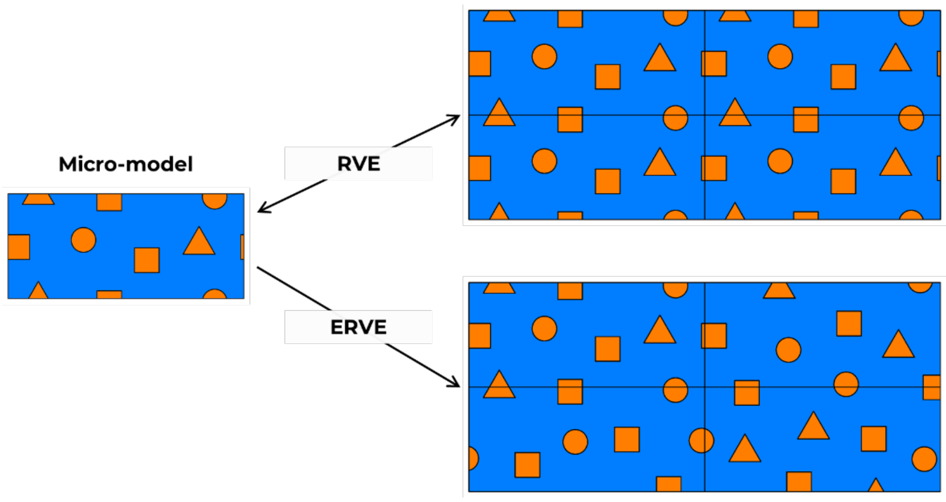

Figure 2. Implications of using a micro-model as a RVE or as an ERVE

2.3 Damage constitutive law

In order to account for material failure, composite constituents must be characterized with a law that provides their elastic behaviour, and also their mechanical response after reaching their failure threshold. The two formulations aforementioned are capable of using any constitutive model to characterize the composite constituents. Among the different models available in literature, this work uses the Katchanov explicit isotropic damage model [45], [46]. This model has been already used with both formulations to characterize composite failure, providing excellent results as it is shown in [24], [35], [42].

An isotropic damage formulation is based in the introduction of a scalar internal variable, the damage parameter d, that considers the reduction of the effective area of the material by reducing its stiffness. The damage variable takes values ranged between 0 and 1, being zero when the material is not damaged and one when the material is completely degraded. The damage parameter is used to transform the real damaged stress tensor, σ, into an effective stress tensor, σ_0. The relation between the damaged stress and the strain in the material depends on the damage parameter and the elastic stiffness tensor (C_0):

$$\sigma \equiv (1-d)\,\sigma_0 = (1-d)\,C_0 : \varepsilon_0 \tag{5}$$

which is rewritten in indicial notation as:

$$\sigma_{ij} \equiv (1-d)\,C_{0_{ijkl}}\,\varepsilon_{0_{kl}} \tag{6}$$

The constitutive model requires the definition of a threshold law, which must provide the stress level at which material degradation starts, as well as the evolution of the damage parameter during the failure process. This law is usually written with the following expression [45]:

$$F(\sigma_0, d) = f(\sigma_0) - c(d) \le 0 \tag{7}$$

being $F(\sigma_0, d)$ the function used to define the damage surface, which is divided in a function depending on the effective stress tensor, $f(\sigma_0)$, and a function depending on the damage parameter, $c(d)$. Damage starts the first time that the value of the effective stress tensor is larger than $c(d)$; and damage evolution is defined by the expression given to this last function.

In current work, the damage surface is defined by the norm of the principal stresses. The variation of the damage parameter is obtained using the damage consistency parameter and the Kuhn-Tucker condition. The law used to define this evolution is exponential and depends, among other parameters, on the fracture energy of the material, G_c. When using a finite element formulation to solve the problem, this material parameter has to be regularized by the fracture length of the element, l_f, in order to obtain mesh independency [24], [47].

$$d = G(f(\sigma_0)) = 1 - \frac{\sigma_{max}}{f(\sigma_0)} e^{A\left(1-\frac{f(\sigma_0)}{\sigma_{max}}\right)};\ \text{ with } A = \frac{1}{\frac{G_c\,C_0}{l_f\,\sigma_{max}^2} - \frac{1}{2}} \tag{8}$$

2.4 Anisotropy using a mapping space theory

This theory is based on the transport of all the constitutive parameters and the stress and strain states of the structure, from the real anisotropic space, to a fictitious isotropic space. Once all variables are in the fictitious isotropic space, an isotropic constitutive model can be used to obtain the new structure configuration. This theory allows considering materials with high anisotropy, such as composite materials, using all techniques and procedures already developed for isotropic materials.

All the anisotropy information is contained in two fourth order tensors. One of them, A^{σ}_{ijkl} , relates the stresses in the fictitious isotropic space ($\bar{\sigma}_{ij}$) with the stresses in the real anisotropic space (σ_{ij}) and the other one, A^{ε}_{ijkl} , does the same with the strains. The relation of both spaces for the strains and the stresses is described in the following equation:

$$\begin{aligned} \bar{\sigma}_{ij} &= A^{\sigma}_{ijkl}\,\sigma_{kl} \\ \bar{\varepsilon}_{ij} &= A^{\varepsilon}_{ijkl}\,\varepsilon_{kl} \end{aligned} \tag{9}$$

A representation of these transformations is displayed in Figure 3. A more detailed description of this methodology, its extension to large strains, and its numerical implementation can be obtained in references [48] and [49].

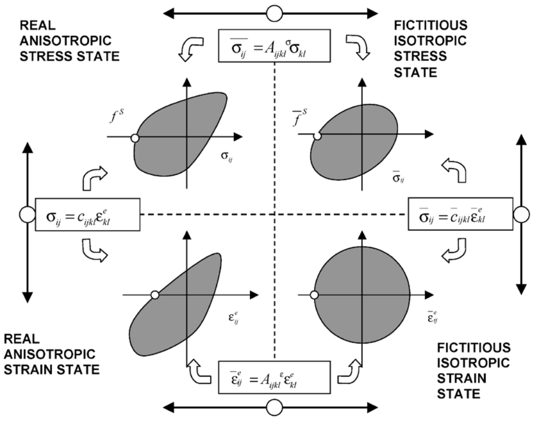

Figure 3. Anisotropy using a mapping space theory. Space transformations. Real and fictitious stress and strain spaces. [48]

3 NONWOVEN FLAX BIOCOMPOSITES

As it has been previously stated, this work focuses on nonwoven eco-composites, as the complexity of their internal microstructure is perfect to test the capabilities of the proposed formulations. Of the different bio-based nonwoven composites available in the market, the particular case of an epoxy matrix with embedded flax fibres will be studied.

3.1 Flax non-woven samples

The nonwoven flax samples were manufactured at the German Aerospace Centre (DLR) in Braunschweig, as a part of a broader experimental campaign, which is fully described in [5]. The nonwoven composite was produced with flax fibres that were obtained from the company INTERCOT in Spain, and a thermoset matrix system obtained from the two-component liquid epoxy infusion resin Hexion Epikote™ RIMR135 with curing agent RIMH1366. The composites were produced with the single line infusion (SLI) method in a Lauffer hydraulic press (500 mm × 500 mm pressing area). The SLI process is characterised by using the same line for vacuum generation followed by the liquid resin infusion. Curing time in the heated hydraulic press was 120 min at 85°C followed by deforming and post-curing at 100°C for 60 min in a Memmert UFP500 convection oven. After cutting, ultrasonic testing in water were carried out to assess the laminate quality regarding pore distribution and delamination. The physical properties of the composites are summarized in Table 1.

Laminate	Fibre Volume Content [%]	Average Thickness [mm]	Density [g/cm³]	Void Content [%]	Glass Transition Temp. [°C]	Water Content [%]
30Flax	29.1	3.11	1.16	7.7	82.3	1.94

Table 1. Physical properties of the nonwoven flax composites produced.

Figure 4a shows the raw flax fibres, Figure 4b shows these same fibres after carding. With the carding procedure it is possible to provide some preferred orientation to the material. Finally, Figure 4c shows the final nonwoven eco-composite once the resin has been infused.

(a)  (b) 

(c) 

Figure 4. Nonwoven flax fibres in the different phases of the manufacturing process. (a) Raw flax fibres. (b) Flax fibres after carding proces. (c) Nonwoven flax composite after infusing the resin, cut for flexural testing. These images have been obtained from the work conducted by DLR in WP2 of Eco-compass project.

3.2 Experimental campaign

Four-point flexural tests were carried out according to the standard DIN EN ISO 14125 (class II, l/h ≅ 20) on a Zwick Roell universal testing machine Z005. A strain rate of 2 mm/min was used with a load cell of 5kN (type KAF-Z, Zwick Roell GmbH & Co KG, Germany). Strain was measured by cross-head displacement. Test samples were sawed to 60 mm length and 15 mm width (b_0) in 0° and 90° laminate direction on a KKS 1300 C (MAIKO Engineering GmbH). A span-to-depth ratio of 20:1 at a laminate thickness (t_0) of 3 mm was chosen in this study because of the limited available number of specimens. The relatively low span-to-depth ratio can cause shear stresses resulting in additional displacements and therefore a potentially lower modulus [50]. Flexural modulus (E_{4PB}) was calculated with the secant method between 0.05 % and 0.25 % strain. The results obtained for the five samples tested are described in Table 2. The stress-strain graphs obtained are shown in Figure 5.

#	t_0 [mm]	b_0 [mm]	F_{max} [N]	D_{max} [mm]	ε_{max} %	σ_{4PB} [MPa]	E_{4PB} [MPa]
1	3.07	15.29	256.31	6.33	3.64	89.11	4589.54
2	3.09	15.35	274.29	6.78	3.92	93.76	4808.43
3	3.1	15.25	253.83	6.58	3.82	86.77	4470.80
4	3.07	15.33	246.18	6.33	3.63	85.36	4322.54
5	3.01	15.13	230.61	6.03	3.40	84.28	4515.47
Average	**3.07**	**15.27**	**252.24**	**6.41**	**3.68**	**87.86**	**4541.36**

Table 2. Results obtained from the experimental campaign conducted on nonwoven flax composites. The values shown in the table are t_0: specimen thickness, b_0: specimen width, F_{max}: maximum force at failure, D_{max}: maximum displacement at failure, ε_{max}: maximum strain at failure, σ_{4PB}: calculated stress at failure, and E_{4PB}: calculated young modulus.

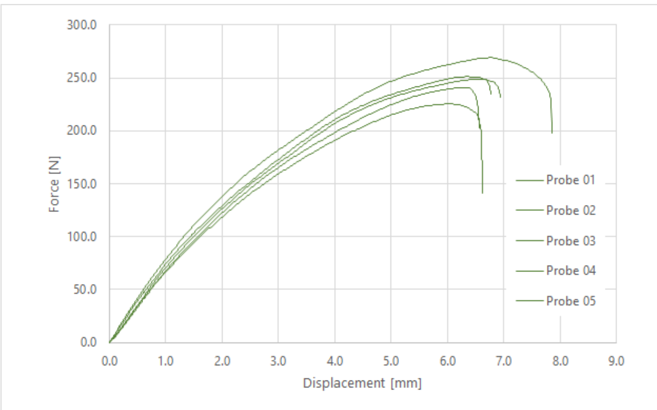

Figure 5. Experimental results of 3PB flax tests. Each Probe curve corresponds to a sample tested.

4 COUPLING HOMOGENIZATION METHODS. ANALYSIS OF FLAX NONWOVEN COMPOSITES

As it has been stated in the introduction, this work proposes a novel methodology to simulate the mechanical performance of nonwoven bio-composites. This is achieved by combining the two homogenization processes described in section 2 of this manuscript: the serial-parallel mixing theory and a numerical homogenization method. The coupling of these two formulations is based on three different assumptions, or hypothesis, that are defined in the following. Afterwards, this section illustrates how the proposed methodology can be applied. This is done with the analysis of the nonwoven flax biocomposite described in section 3.

4.1 Coupling hypothesis

The complexity of the internal microstructure of nonwoven flax eco-composites requires of a multiscale procedure to account for the interaction between the different composite constituents. However, the size of the micro-model required to represent the internal microstructure of the composite makes unaffordable the solution of the whole problem using only multiscale methods. For this reason, it is proposed to couple both formulations available, the serial-parallel mixing theory and the numerical multiscale procedure. This coupling is made based on three main hypotheses:

1. The randomness in the orientation of the fibre distribution that presents the nonwoven composite can be captured by considering that there are different composite materials, or composite layers, with a preferred orientation, all of them sharing the same strains (iso-strain condition)
2. Inside each one of these composite materials, the interaction between fibre and matrix is accounted with the serial-parallel mixing theory, assuming an iso-strain performance in the fibre direction and an iso-stress performance in all other directions
3. Fibre curviness and its effect over the composite performance is accounted by modifying the mechanical properties of fibre and matrix materials. The modifications required are obtained from a numerical multiscale analysis made on an Equivalent Representative Volume Element (ERVE).

4.2 Coupon model developed

4.2.1 Model geometry and boundary conditions

The performance of the nonwoven flax composite has been studied by conducting four-point bending (4PB) tests on the material, which are defined in the standard ISO 14125:2011-05. The capacity of the formulation developed to characterize the material performance will be tested by reproducing this 4PB test. The sample dimensions are shown in Figure 6a, while the test configuration and its dimensions are plotted in Figure 6b. These dimensions are in accordance with the dimensions reported from the experimental campaign (Table 2). Figure 6c shows the coupon while it is tested and the displacement transducer used to record the displacements during the test.

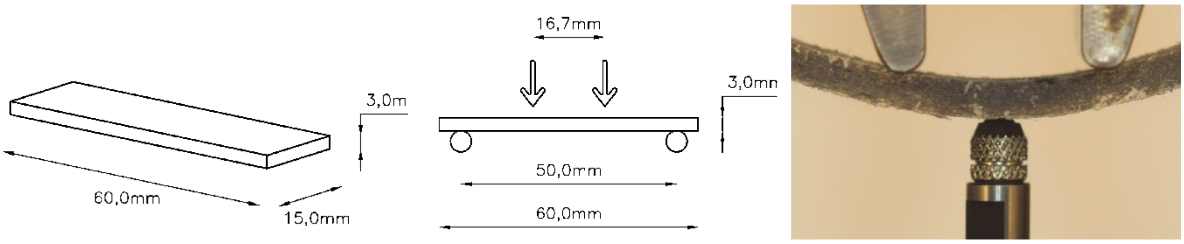

(a) (b) (c)

Figure 6. 4PB test conducted on the nonwoven flax composite. (a) Coupon dimensions. (b) Test configuration and dimensions (c) Photograph of the testing sample, above the sample are the elements that apply the load, below the sample is the displacement transducer.

The numerical model developed to simulate the 4PB test is shown in Figure 7, where it is shown the geometry and the boundary conditions applied to it. The model has been loaded with an imposed displacement (red arrows). The finite element mesh is made with 7920 quadratic hexahedra elements.

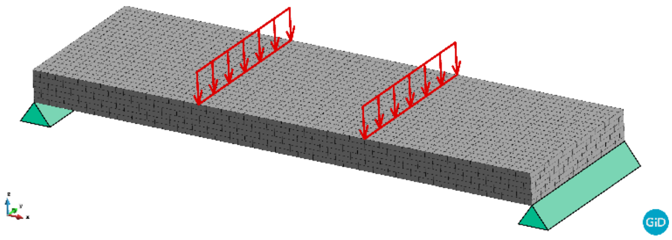

Figure 7. Numerical model developed to simulate the 4PB test conducted on the nonwoven flax composite.

4.2.2 Materials defined in the model

The experimental coupon is made of flax fibres embedded in an epoxy matrix. The matrix used is the Epikote^{TM} resing MGS^{TM} RIMR135 manufactured by Hexion. Its main mechanical parameters are provided by the manufacturer and are listed in Table 3. As for flax fibres, its main mechanical parameters have been obtained from the work conducted in references [51] and [52], due to the lack of data available from the manufacturer. These properties are also listed in Table 3. As for the Poisson value given to flax fibers, the value provided by the referred publications is close to 0.5 (0.498) [51]. This value has been reduced to 0.4 to avoid incompressibility problems in the numerical analysis.

	Epikote Epoxy	Flax Fibres
Young Modulus E1 [GPa]	2.7	50
Young Modulus E2 and E3 [GPa]	2.7	8.0
Poisson modulus	0.36	0.40
Tensile strength [MPa]	70	900

Table 3. Main mechanical properties of the flax nonwoven composite constituents

A last parameter that it is required in order to have a complete characterization of the composite material is the volumetric participation of fibre and matrix in the composite. For current nonwoven, the proportions that where measured by DLR in their experimental campaign were 29.1% of flax fibres and 70.9% of epoxy resin (the void content described in Table 1 has been assigned to the epoxy resin).

Besides the material mechanical parameters, it is necessary to take into account other material properties such as fibre orientation and curviness. As it has been stated in the model hypothesis (section 4.1), fibre orientation will be accounted by defining different composite materials with different fibre orientations, and assuming that all of them have the same strain tensor. The composite stress will be obtained according to the volumetric participation of each material in the composite. Therefore:

$$\begin{gathered}\varepsilon_{composite} = \varepsilon_{\theta 1} = \varepsilon_{\theta 2} = \cdots = \varepsilon_{\theta n} \\ \sigma_{composite} = k_{\theta 1}\,\sigma_{\theta 1} + k_{\theta 2}\,\sigma_{\theta 2} + \cdots + k_{\theta n}\,\sigma_{\theta n}\end{gathered} \tag{10}$$

The value n depends on the discretization made on the angle spectra that these materials can take. In current simulations, the space ranging from -90º to +90º has been divided in 12 segments, with angle variations every 15º. The volumetric participation that has to be assigned to each angle allows considering the efficiency of the carding treatment done to the flax fibres before infusing the matrix. If the carding has been effective, there will be a larger participation of materials oriented around 0º than if the carding has not been effective. Following a visual inspection of the non-woven samples, this work assumes a random distribution of the fibre orientation in the composite, which is defined assigning the same volumetric participation to all segments.

The interaction between flax fibres and the epoxy matrix for each one of these materials is taken into account with the serial-parallel mixing theory, assuming an iso-strain condition in the fibre direction and an iso-strain condition in all other directions. This formulation provides an excellent prediction of the material performance when it is applied to unidirectional laminate composites, as it is proved in the simulations conducted in references [23]–[25], [53]. However, if this formulation is applied to nonwoven composites, it does not take into account the effect of fibre curviness and it predicts very large stiffness values, compared to the actual stiffness measured in the material. To overcome this limitation, this work proposes to modify the mechanical properties of fibre and matrix, based on the results obtained with a micro-model of the composite. With the modified properties, the the serial parallel mixing theory should provide the same mechanical response than the micro-model.

4.3 Equivalent Representative Volume Element (ERVE) of a curved flax fibre in an epoxy matrix

This work uses an Equivalent Representative Volume Element to obtain the mechanical performance expected from the non-woven flax composite. The ERVE considered is the one represented in Figure 8. This is obtained by reproducing the exact geometry of three different flax fibres existing in the actual material. Fibres have been selected having a preferred orientation, as this material is the one that will be rotated afterwards to consider the randomness in fibre direction of the composite. The number of fibres included in the ERVE, as well as the waviness of these fibres, have been defined in order to obtain an average representation of the material.

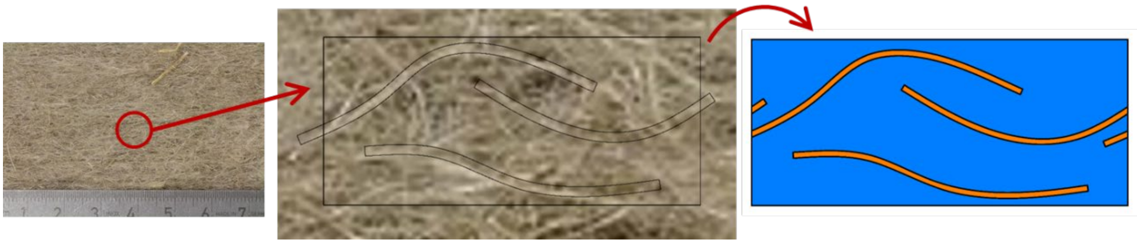

Figure 8. Geometry of the Equivalent Representative Volume Element (ERVE) developed to study the mechanical performance of nonwoven flax composites

This is considered a good example of the requirements of an ERVE, and the results expected from it. In this analysis, the results expected from the ERVE are the effect of the length and curviness of flax fibres in the composite, therefore it is possible to simplify the geometry of the model to reduce its computational cost.

The properties assigned to the epoxy matrix and the flax fibres of the micro-model are those defined in Table 3. This micro-model has been applied to a macro-model geometry which has been loaded with a longitudinal tensile load and a transversal tensile load, in order to obtain the material performance. The results obtained and the procedure followed to apply these results to the mechanical analysis of the 4PB test of the nonwoven flax composite are described in the following section.

5 RESULTS OBTAINED FROM THE NUMERICAL ANALYSIS

The first numerical analyses are made on the ERVE multiscale model, in order to obtain the equivalent properties that have to be assigned to the flax fibres and the epoxy matrix in the serial-parallel mixing theory to account for the flax curviness. With the results obtained from this first analysis it is possible to conduct the 4PB test described in previous section, using the serial-parallel mixing theory, in order to obtain the flax nonwoven composite performance. The results obtained from the different numerical models developed are detailed hereafter, following the same order required to conduct them.

5.1 Micro-model analysis

The Equivalent Representative Volume Element developed to analyse the mechanical performance of the flax-epoxy composite, accounting for fibre curviness, is the one shown in Figure 8. The multiscale scheme followed to obtain the performance of the micro-model is depicted in Figure 9, that shows the macro-structure and the RVE defined. The macro-model is defined only with three finite elements as its main function is to apply the loads to the micro-model and to obtain its response. The use of a larger model will increase substantially the computational cost and will provide the same results. Two different multiscale analyses have been conducted applying a monotonically increasing load to the material, one with a longitudinal load, corresponding to the X axis in Figure 9, and a second one with a transversal load, corresponding to the Y axis. The first analysis is used to obtain the equivalent stiffness of flax fibres and their equivalent failure stress. The transversal load analysis has been used to obtain the transversal strength of the epoxy matrix material.

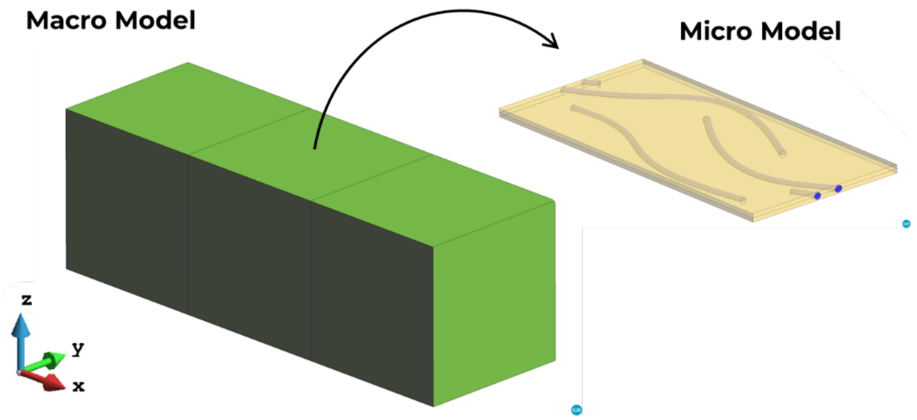

Figure 9. Macro and micro-models used to obtain the equivalent properties of flax fibres. The coordinate system is shared by both models.

5.1.1 *Elastic longitudinal analysis*

Figure 10 shows the longitudinal stresses in the micro-model when a pure longitudinal load is applied to the macro model. This image shows that the maximum stresses are found in the flax fibres, which is an expected result, as they are substantially stiffer than the epoxy matrix. Figure 10 also shows that stresses are not constant along the fibre length, being larger in the sectors in which the fibre orientation is closer to the load direction.

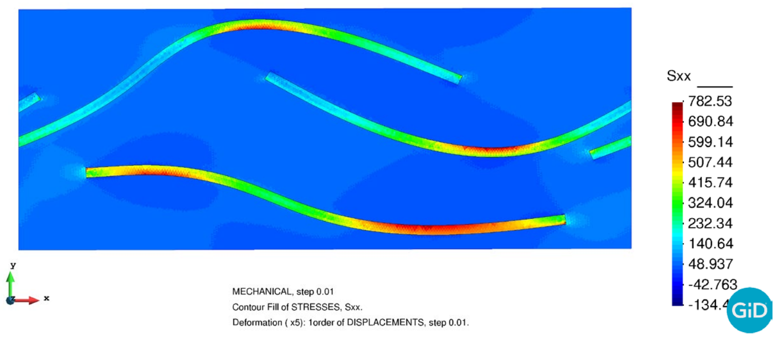

Figure 10. Longitudinal stresses in flax fibres and epoxy matrix under a linear elastic analysis applying a longitudinal load

This first analysis makes possible to obtain the longitudinal stiffness of the composite provided by the ERVE defined. This stiffness has a value of $E_{RVE} = 3741\ MPa$.

If this same elastic performance has to be reproduced with the serial-parallel mixing theory, it is necessary to modify the fibre elastic stiffness in such a way that, with the same volumetric participation of fibre and matrix, the stiffness of the composite is the one provided by the ERVE. The volumetric participation of matrix and fibre in the ERVE defined is, $k^m = 0.941$ and $k^f = 0.059$, respectively. Knowing that in the longitudinal direction the serial-parallel mixing theory obtains the composite stiffness assuming a parallel performance:

$$E_{RVE} = k^f\ E_f + k^m\ E_m \tag{11}$$

and assuming that the matrix stiffness remains equal in both models, of $E_m = 2700 MPa$, it is possible to obtain the equivalent stiffness required for flax fibres:

$$E_f = \frac{E_{RVE} - k^m\ E_m}{k^f} = 20344\ MPa \tag{12}$$

5.1.2 Non-linear longitudinal analysis

The same model presented previously has been solved with an increasing longitudinal load using a damage formulation to characterize both constituent materials, fibre and matrix. The load has been applied with an imposed displacement in one of the sides of the macro-model. The maximum displacement reached by the model is 0.075mm, which corresponds to a load of 93.5N. This is shown in Figure 13. The five first displacement increments are of 0.01mm while the following ones are of 0.001 in order to facilitate the convergence of the problem. The stress threshold applied to the materials is the one defined in Table 3. The damage parameter obtained at the end of the simulation is shown in Figure 11. This figure shows that most of the damage is concentrated at the tip of flax fibres, mainly produced by normal stresses. There is also substantial damage around the fibres contour, this one produced by the shear forces induced due to the different stiffness between fibres and matrix.

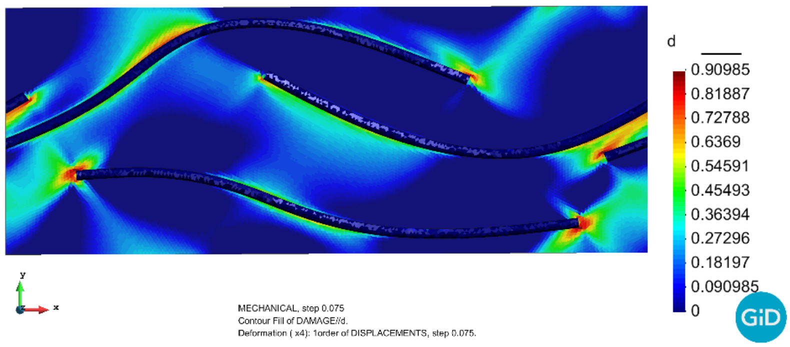

Figure 11. Damage parameter produced by longitudinal loads in the flax nonwoven ERVE under study

Figure 12 shows that although it is not possible to see it properly in Figure 11, fibres have also reached their threshold stress when the maximum load is applied to the representative volume element.

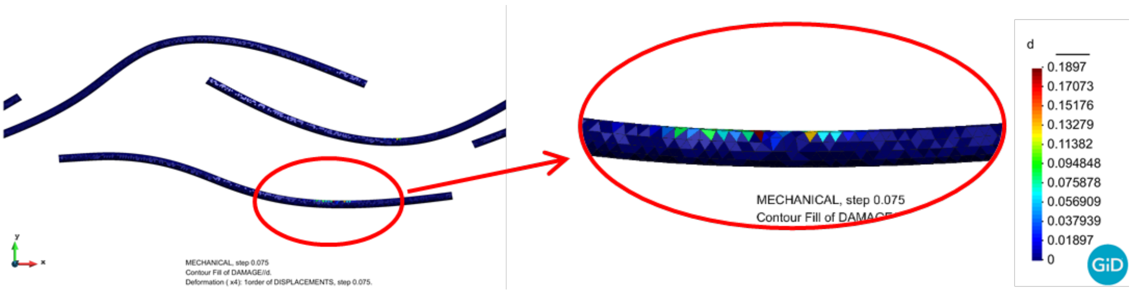

Figure 12. Damage parameter in the RVE analyzed to study the performance of the flax nonwoven composite

These results show that the composite failure is produced when its components reach their maximum stress level, and that these stresses are result of a combination of micro-structural effects. The serial-parallel mixing theory is not capable of reproducing these sort of material interactions, therefore it is necessary to simplify this failure mode. This is done considering that the longitudinal failure of the composite is produced by fibre failure, and reducing the fibre tensile strength from 900MPa to 500MPa. With this approach, the mechanical response of the micro-model and the serial-parallel mixing theory is equivalent, as it is shown in Figure 13. This figure shows the force-displacement graphs obtained for a material sample of identical dimensions, one analysed with the multiscale model and the other one with the serial-parallel mixing theory. Figure 13 also shows that the serial parallel mixing theory model is capable to describe the softening of the material, as the response provided by this model comes from the combination of two damage laws, while the micro-model loses convergence when it reaches its stress threshold. This sudden loss of convergence is because the level of damage in the ERVE at this point is close to one in several elements (Figure 11). Another comparison that is worth doing of these two models is their computational cost: while the serial-parallel model runs in less than 0.4 seconds, the multiscale model has required 1h and 18minutes to run the simulation. This high computational cost is consequence of the large mesh required to simulate properly the ERVE, and is the main reason that makes unfeasible considering these sort of analysis with a pure multiscale procedure.

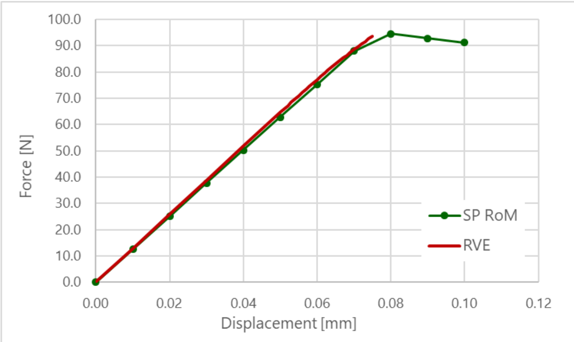

Figure 13. Comparison of the mechanical performance of the multiscale analysis and the analyisis made with the serial-parallel mixing theory of a small coupon of flax nonwoven composite

5.1.3 Non-linear transversal analysis

The multiscale model has also been used to obtain the mechanical performance of the flax-epoxy ERVE when it is subjected to transversal loads. The load applied has been increased monotonically until reaching the material failure. As in the longitudinal analysis, the load has been applied by imposing a fixed displacement. The final displacement reach by the model is of 0.081mm, which corresponds to a load of 82.6N. The first five displacement increments are of 0.01mm, these are followed by five increments of 0.005mm and by three last increments of 0.002mm. The results obtained from this simulation are shown in Figure 14 in terms of the damage parameter in the composite components. This figure shows that the composite failure is produced by the rupture of the fibre-matrix interface, as a result of matrix failure. Therefore, the transversal strength of matrix material will be defined based on this interfacial strength. Several authors have studied experimentally this phenomena [54]–[56], finding out that the interfacial strength between flax fibres and an epoxy matrix is around 20 and 30 MPa. Using these values obtained from literature, this work defines the transversal strength of the epoxy resin at 20 MPa.

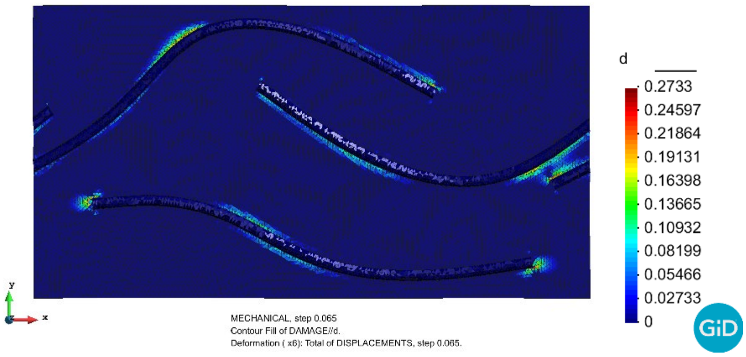

Figure 14. Damage parameter produced by transversal loads in the flax nonwoven ERVE under study

5.2 Macro-model analysis. 4PB Test of a flax nonwoven composite

The 4PB test analysed in this section replicates the experimental campaign conducted at DLR and described in section 3.2. The dimensions of the sample and the loads applied are depicted in Figure 6 and in Figure 7. The load has been applied by imposing a vertical displacement with constant increments of 0.1mm. As previously stated, the results obtained from the different multiscale simulations conducted have been used to modify the material parameters of flax fibre and epoxy matrix. The new values are shown in Table 4. These values are the ones that will be applied to the serial-parallel mixing theory model in order to characterize the mechanical response of the flax nonwoven composite. The different strength values shown in Table 4 for the epoxy material will be applied with the anisotropy using the mapping space formulation defined in section 2.4. The rest of the model properties, such as fibre orientation, dimensions, loads applied, etc. have been already described in section 4.2.

	Epikote Epoxy	Flax Fibres
Young Modulus E1 [GPa]	2.7	20.3
Young Modulus E2 and E3 [GPa]	2.7	8.0
Poisson modulus	0.36	0.40
Longitudinal strength [MPa]	70	500
Transversal strength [MPa]	20	500

Table 4. Modified mechanical properties for the numerical analysis of the flax nonwoven composite constituents

The results obtained with the numerical model developed for the Four Point Bending (4PB) test conducted on the flax nonwoven composite are shown in the following figures. Figure 15 shows the stress field in the displaced model of the tested coupon. This result shows that the 4PB test boundary conditions are properly applied, as the deformation and the stress field are the ones expected.

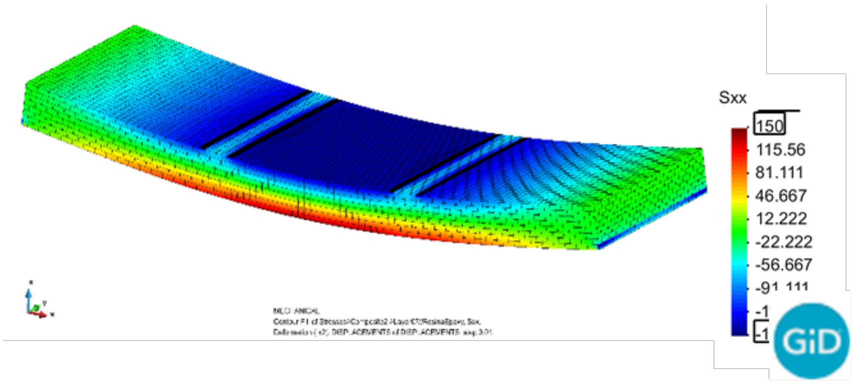

Figure 15. Deformation and stresses obtained for the numerical model of the 4PB test made on flax nonwoven composite

The serial-parallel mixing theory obtains the composite behaviour from its constituents; therefore, the model has information on the performance of the fibres and the resin at the different orientations defined. This allows obtaining a detailed description of the failure mechanisms of the specimen. This failure is shown by means of the damage parameter in the resin and the flax fibres in Figure 16 and Figure 17, respectively. In these two figures, the regions in which the boundary conditions are applied are not depicted because these regions have large stress concentrations that do not allow a correct visualization of the whole structure performance.

Figure 16 shows the damage parameter in the epoxy resin associated to different fibre orientations, at the last step of the numerical analysis before failure. This figure shows that most of the matrix is completely damaged, with damage values above 0.9 for nearly all fibre orientations. This figure also shows that the resin associated to fibres at 90º have a slightly larger damage than those associated to 0º. This is coherent with the fact that the transversal strength of the resin is defined with a lower value than the longitudinal strength.

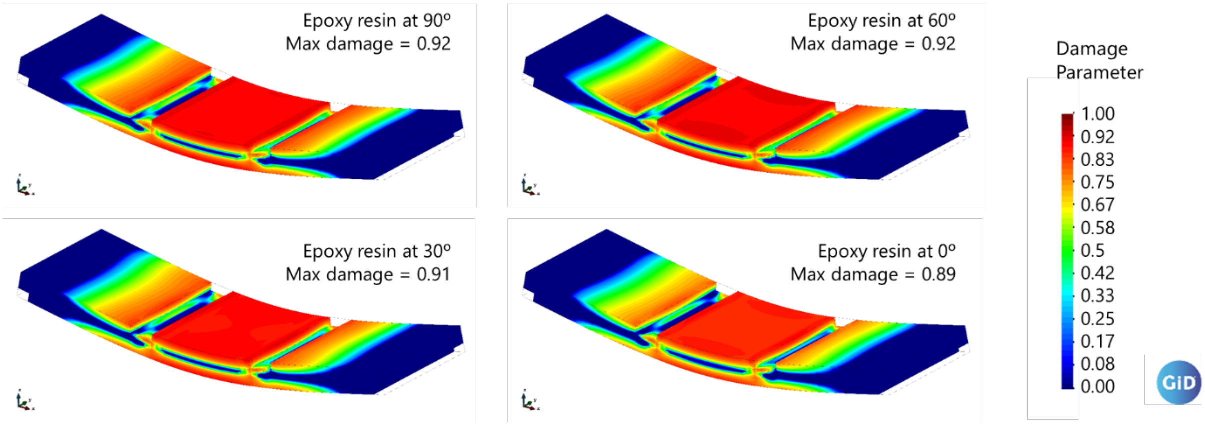

Figure 16. Damage parameter in the resin associated to different fibre orientations at the last load step applied to the numerical model.

Figure 17 shows the damage parameter in the fibres for different orientations at the last load step. In this case it can be seen that the fibres with larger damage are those at 0º, which are oriented following the direction of maximum stresses. As the fibre orientation increases towards 90º, fibre damage decreases and becomes zero for orientations larger than 45º. It is worth noting that having the fibres more aligned with the principal stresses in the structure implies having larger damage, and also implies to have a larger extension of fibres with damage.

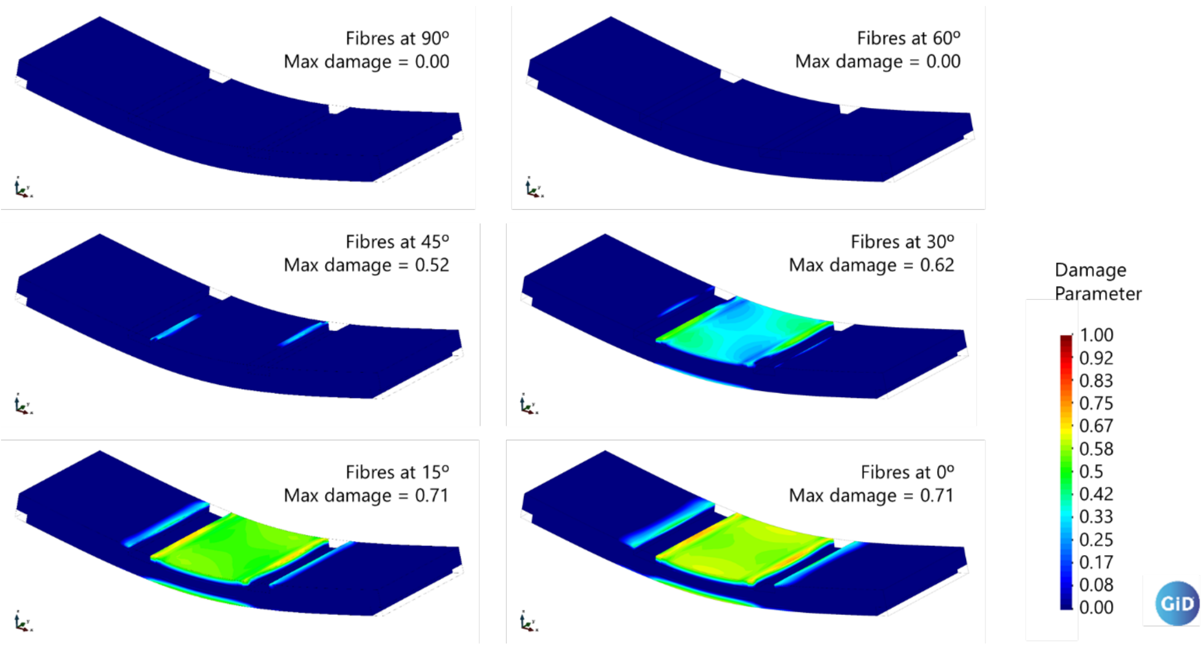

Figure 17. Damage parameter in the flax fibres at different fibre orientations at the last load step applied to the numerical model.

The comparison of the results provided by the numerical model with the results obtained in the experimental campaign is made using the force-displacement graph. The force corresponds to the total vertical load applied to the sample, and the displacement is measured at mid span. This result comparison is shown in Figure 18. This figure shows a complete agreement between the numerical and the experimental results. The initial stiffness provided by the numerical model matches perfectly the stiffness measured in the tested coupons. The material shows a variation of this stiffness for an applied force close to 100N, providing a non-linear behaviour for larger loads. The maximum load that can be applied to the coupon in the numerical model is around 250N (258.5N, to be exacts) which, again, fits in the maximum loads range provided by the experimental campaign. The failure of the numerical model is reached for a displacement of 6.1mm, at this point the matrix in damage is larger than 0.9 in most elements, as it is shown in Figure 16, and the model cannot reach convergence. It is also worth noting that the experimental failure is very abrupt, once the maximum load is reached, which corresponds to the loss of convergence reached by the numerical model.

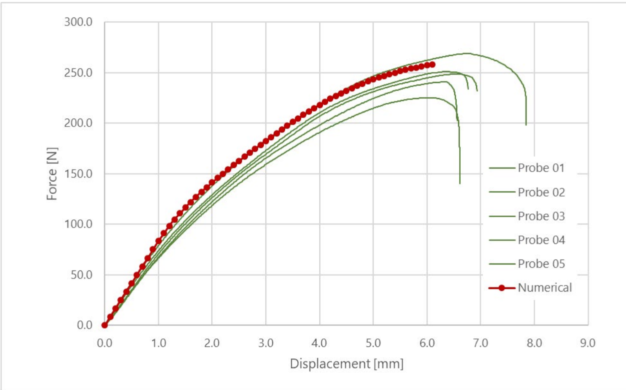

Figure 18. Force displacement graph obtained for the numerical model and the experimental test of the 4PB test made on flax nonwoven composite. Probe 01 to Probe 05 curves correspond to the results obtained from the experimental campaign.

6 CONCLUSIONS

The prediction of the mechanical performance of composites with complex microstructures, such as the flax nonwoven biocomposites reported in this work, can be approached by empirical formulations mostly based in experimental results; or can be conducted with complex simulation procedures, such as multiscale methods, in order to account for the different interactions that take place among their components. The main drawback of this last approach is the computational cost required to conduct the simulation. Therefore, simplified methods are needed to obtain an accurate prediction of the composite performance.

This work has presented a novel methodology that combines two different homogenization procedures for the analysis of nonwoven biocomposites. The analysis of the composite structure is conducted with the Serial-Parallel mixing theory, which uses modified material properties based on the results obtained from a numerical multiscale analysis. With the proposed methodology, it is possible to account for the complex micro-structural interactions of the composite constituents, such as the effect of fibre waviness or the nonwoven failure mechanisms, with an affordable computational cost. This feature, together with the possibility to know at each load step the current stress-strain state of the composite components, are some of the advantages provided by the proposed approach compared to other procedures that only provide the global response of the laminate.

One of the implications of the developed procedure is that it has been necessary to modify and extent the concept of RVE to what has been defined as an Equivalent Representative Volume Element (ERVE). An ERVE is not a reduced model of a periodic material that fulfils the scale separation criteria, but instead is a numerical model of the material, which is capable of providing a similar mechanical response in terms of stiffness and failure modes. The ERVE is an equivalent model that provides the material response, not a real representation of the material itself. In fact, the configuration defined for the ERVE may not exist in the material itself.

The procedure proposed, although it has been applied to a flax nonwoven biocomposites, can be applied to other composites with complex internal microstructures. When applied to the nonwoven biocomposite described in this work, the numerical analysis conducted has provided excellent results when compared with the experimental tests obtained from the manufactured samples. The agreement between the numerical and experimental results, not only validate the methodology proposed, but they have also provided a better understanding on the mechanical performance of these composites, which will facilitate their use in different engineering structures, improving their environmental footprint.

Acknowledgements

This work has received funding from the European Union's Horizon 2020 research and innovation program under grant agreement No 690638, from the Special Research Plan on Civil Aircraft of Ministry for Industry and Information of the People's Republic of China (MIIT) under Grant No MJ-2015-H-G-103, and from the Spanish Ministerio de Economia y Competividad through the project MAT2014-60647-R, Multi-scale and multi-objective optimization of composite laminate structures (OMMC). All this support is gratefully acknowledged.

REFERENCES

[1] A. Lefeuvre, S. Garnier, L. Jacquemin, B. Pillain, and G. Sonnemann, "Anticipating in-use stocks of carbon fiber reinforced polymers and related waste flows generated by the commercial aeronautical sector until 2050," *Resour. Conserv. Recycl.*, vol. 125, pp. 264–272, Oct. 2017.

[2] S. Karuppannan Gopalraj and T. Kärki, "A review on the recycling of waste carbon fibre/glass fibre-reinforced composites: fibre recovery, properties and life-cycle analysis," *SN Appl. Sci. 2020 23*, vol. 2, no. 3, pp. 1–21, Feb. 2020.

[3] A. Regazzi *et al.*, "Microstructural and mechanical properties of biocomposites made of native starch granules and wood fibers," *Compos. Sci. Technol.*, vol. 182, p. 107755, Sep. 2019.

[4] V. Mazzanti, R. Pariante, A. Bonanno, O. Ruiz de Ballesteros, F. Mollica, and G. Filippone, "Reinforcing mechanisms of natural fibers in green composites: Role of fibers morphology in a PLA/hemp model system," *Compos. Sci. Technol.*, vol. 180, pp. 51–59, Aug. 2019.

[5] J. Bachmann, M. Wiedemann, and P. Wierach, "Flexural Mechanical Properties of Hybrid Epoxy Composites Reinforced with Nonwoven Made of Flax Fibres and Recycled Carbon Fibres," *Aerosp. 2018, Vol. 5, Page 107*, vol. 5, no. 4, p. 107, Oct. 2018.

[6] L. Mohammed, M. N. M. Ansari, G. Pua, M. Jawaid, and M. S. Islam, "A Review on Natural Fiber Reinforced Polymer Composite and Its Applications," *Int. J. Polym. Sci.*, vol. 2015, 2015.

[7] J. Bachmann *et al.*, "Outlook on ecologically improved composites for aviation interior and secondary structures," *CEAS Aeronaut. J. 2018 93*, vol. 9, no. 3, pp. 533–543, Apr. 2018.

[8] J. Bachmann *et al.*, "Towards a Circular Economy in the Aviation Sector Using Eco-Composites for Interior and Secondary Structures. Results and Recommendations from the EU/China Project ECO-COMPASS," *Aerosp. 2021, Vol. 8, Page 131*, vol. 8, no. 5, p. 131, May 2021.

[9] J. P. Torres, L.-J. Vandi, M. Veidt, and M. T. Heitzmann, "The mechanical properties of natural fibre composite laminates: A statistical study," *Compos. Part A Appl. Sci. Manuf.*, vol. 98, pp. 99–104, Jul. 2017.

[10] K. L. Pickering, M. G. A. Efendy, and T. M. Le, "A review of recent developments in natural fibre composites and their mechanical performance," *Compos. Part A Appl. Sci. Manuf.*, vol. 83, pp. 98–112, Apr. 2016.

[11] V. Gigante, L. Aliotta, V. T. Phuong, M. B. Coltelli, P. Cinelli, and A. Lazzeri, "Effects of waviness on fiber-length distribution and interfacial shear strength of natural fibers reinforced composites," *Compos. Sci. Technol.*, vol. 152, pp. 129–138, Nov. 2017.

[12] C. L. Pai, M. C. Boyce, and G. C. Rutledge, "On the importance of fiber curvature to the elastic moduli of electrospun nonwoven fiber meshes," *Polymer (Guildf).*, vol. 52, no. 26, pp. 6126–6133, Dec. 2011.

[13] Y. He, N. Deng, B. Xin, and L. Liu, “3D microstructure reconstruction of nonwoven fabrics based on depth from focus,” *Micron*, vol. 144, May 2021.

[14] Z. Qiu and H. Fan, “Nonlinear modeling of bamboo fiber reinforced composite materials,” *Compos. Struct.*, vol. 238, p. 111976, Apr. 2020.

[15] M. Zhang, W. Lu, P. I. Gouma, Z. Xu, and L. Wang, “Theoretical prediction of effective stiffness of nonwoven fibrous networks with straight and curved nanofibers,” *Compos. Part A Appl. Sci. Manuf.*, vol. 143, p. 106311, Apr. 2021.

[16] F. Farukh, E. Demirci, B. Sabuncuoglu, M. Acar, B. Pourdeyhimi, and V. V. Silberschmidt, “Mechanical behaviour of nonwovens: Analysis of effect of manufacturing parameters with parametric computational model,” *Comput. Mater. Sci.*, vol. 94, no. C, pp. 8–16, Nov. 2014.

[17] F. Farukh, E. Demirci, B. Sabuncuoglu, M. Acar, B. Pourdeyhimi, and V. V. Silberschmidt, “Mechanical analysis of bi-component-fibre nonwovens: Finite-element strategy,” *Compos. Part B Eng.*, vol. 68, pp. 327–335, Jan. 2015.

[18] C. Naili, I. Doghri, T. Kanit, M. S. Sukiman, A. Aissa-Berraies, and A. Imad, “Short fiber reinforced composites: Unbiased full-field evaluation of various homogenization methods in elasticity,” *Compos. Sci. Technol.*, vol. 187, p. 107942, Feb. 2020.

[19] F. Greco, P. Lonetti, R. Luciano, P. Nevone Blasi, and A. Pranno, “Nonlinear effects in fracture induced failure of compressively loaded fiber reinforced composites,” *Compos. Struct.*, vol. 189, pp. 688–699, Apr. 2018.

[20] F. Levrero-Florencio, L. Margetts, E. Sales, S. Xie, K. Manda, and P. Pankaj, “Evaluating the macroscopic yield behaviour of trabecular bone using a nonlinear homogenisation approach,” *J. Mech. Behav. Biomed. Mater.*, vol. 61, pp. 384–396, Aug. 2016.

[21] F. Levrero-Florencio and P. Pankaj, “Using non-linear homogenization to improve the performance of macroscopic damage models of trabecular bone,” *Front. Physiol.*, vol. 9, no. MAY, p. 545, May 2018.

[22] B. Werner, M. Ovesy, and P. K. Zysset, “An explicit micro-FE approach to investigate the post-yield behaviour of trabecular bone under large deformations,” *Int. j. numer. method. biomed. eng.*, vol. 35, no. 5, p. e3188, May 2019.

[23] F. Rastellini, S. Oller, O. Salomón, and E. Oñate, “Composite materials non-linear modelling for long fibre-reinforced laminates: Continuum basis, computational aspects and validations,” *Comput. Struct.*, vol. 86, no. 9, pp. 879–896, May 2008.

[24] X. Martínez, S. Oller, and E. Barbero, “Study of Delamination in Composites by Using the Serial/Parallel Mixing Theory and a Damage Formulation,” in *Mechanical Response of Composites. Computational Methods in Applied Sciences*, vol. 10, P. P. Camanho, C. G. Dávila, S. T. Pinho, and J. J. C. Remmers, Eds. Dordrecht: Springer, 2008, pp. 119–140.

[25] M. A. Pérez, X. Martínez, S. Oller, L. Gil, F. Rastellini, and F. Flores, “Impact damage prediction in carbon fiber-reinforced laminated composite using the matrix-reinforced mixing theory,” *Compos. Struct.*, vol. 104, 2013.

[26] F. Otero, S. Oller, and X. Martinez, “Multiscale Computational Homogenization: Review and Proposal of a New Enhanced-First-Order Method,” *Arch. Comput. Methods Eng.*, vol. 25, no. 2, pp. 479–505, 2018.

[27] M. Geers, V. G. Kouznetsova, and W. A. M. Brekelmans, “MultiScale First-Order and Second-Order Computational Homogenization of Microstructures towards Continua,” *Int. J. Multiscale Comput. Eng.*, vol. 1, no. 4, pp. 371–386, 2003.

[28] J. A. Hernández, J. Oliver, A. E. Huespe, M. A. Caicedo, and J. C. Cante, “High-performance model reduction techniques in computational multiscale homogenization,” *Comput. Methods Appl. Mech. Eng.*, vol. 276, pp. 149–189, Jul. 2014.

[29] E. J. Barbero, *Introduction to composite materials design*, 3rd Editio. CRC Press, 2017.

[30] C. Truesdell and R. Toupin, “The Classical Field Theories,” Springer, Berlin, Heidelberg, 1960, pp. 226–858.

[31] E. Car, F. Zalamea, S. Oller, J. Miquel, and E. Oñate, “Numerical simulation of fiber reinforced composite materials—two procedures,” *Int. J. Solids Struct.*, vol. 39, no. 7, pp. 1967–1986, Apr. 2002.

[32] L. Neamtu, S. Oller, and E. Oñate, “A generalized mixing theory elasto-damageplastic model for finite element analysis of composites,” in *Complas V - Computational Plasticity*, 1997, pp. 1–5.

[33] X. Martinez, S. Oller, F. Rastellini, and A. H. Barbat, “A numerical procedure simulating RC structures reinforced with FRP using the serial/parallel mixing theory,” *Comput. Struct.*, vol. 86, no. 15–16, pp. 1604–1618, Aug. 2008.

[34] J. J. Granados *et al.*, “Numerical and experimental procedure for material calibration using the serial/parallel mixing theory, to analyze different composite failure modes,” *Mech. Adv. Mater. Struct.*, pp. 1–19, Oct. 2019.

[35] X. Martinez, F. Rastellini, S. Oller, F. Flores, and E. Oñate, “Computationally optimized formulation for the simulation of composite materials and delamination failures,” *Compos. Part B Eng.*, vol. 42, no. 2, 2011.

[36] A. Solis, S. Sanchez-Saez, X. Martinez, and E. Barbero-Pozuelo, “Numerical analysis of interlaminar stresses in open-hole laminates under compression,” *Compos. Struct.*, vol. 217, pp. 89–99, Jun. 2019.

[37] P. SUQUET, “Local and Global Aspects in the Mathematical Theory of Plasticity,” *Plast. Today*, pp. 279–309, 1985.

[38] T. Kanit, S. Forest, I. Galliet, V. Mounoury, and D. Jeulin, “Determination of the size of the representative volume element for random composites: statistical and numerical approach,” *Int. J. Solids Struct.*, vol. 40, no. 13–14, pp. 3647–3679, Jun. 2003.

[39] S. Oller, J. Miquel Canet, and F. Zalamea, “Composite Material Behavior Using a Homogenization Double Scale Method,” *J. Eng. Mech.*, vol. 131, no. 1, pp. 65–79, Jan. 2005.

[40] H. Badillo and S. Oller, “Numerical simulation of composite materials and structures using the unit cell homogenization approach,” in *V international conference on science and technology of composite materials*, 2009.

[41] F. Otero, S. Oller, X. Martinez, and O. Salomón, “Numerical homogenization for composite materials analysis. Comparison with other micro mechanical formulations,” *Compos. Struct.*, vol. 122, 2015.

[42] F. Otero, X. Martinez, S. Oller, and O. Salomón, “An efficient multi-scale method for non-linear analysis of composite structures,” *Compos. Struct.*, vol. 131, 2015.

[43] S. Zaghi, X. Martinez, R. Rossi, and M. Petracca, “Adaptive and off-line techniques for non-linear multiscale analysis,” *Compos. Struct.*, vol. 206, pp. 215–233, Dec. 2018.

[44] S. Nemat-Nasser, “Averaging theorems in finite deformation plasticity,” *Mech. Mater.*, vol. 31, no. 8, pp. 493–523, 1999.

[45] S. Oller, *Nonlinear Dynamics of Structures*. Springer International Publishing, 2014.

[46] J. Oliver, M. Cervera, S. Oller, and J. Lubliner, “Isotropic damage models and smeared crack analysis of concrete,” in *Second international conference on computer aided analysis and design of concrete structures*, 1990, pp. 945–958.

[47] X. Martinez and S. Oller, “Numerical simulation of matrix reinforced composite materials subjected to compression loads,” *Arch. Comput. Methods Eng.*, vol. 16, no. 4, 2009.

[48] E. Car, S. Oller, and E. Oñate, “An anisotropic elastoplastic constitutive model for large strain analysis of fiber reinforced composite materials,” *Comput. Methods Appl. Mech. Eng.*, vol. 185, no. 2–4, pp. 245–277, May 2000.

[49] E. Car, S. Oller, and E. Oñate, “A large strain plasticity model for anisotropic materials — composite material application,” *Int. J. Plast.*, vol. 17, no. 11, pp. 1437–1463, Nov. 2001.

[50] G. Kretsis, “A review of the tensile, compressive, flexural and shear properties of hybrid fibre-reinforced plastics,” *Composites*, vol. 18, no. 1, pp. 13–23, Jan. 1987.

[51] D. Scida, A. Bourmaud, and C. Baley, “Influence of the scattering of flax fibres properties on flax/epoxy woven ply stiffness,” *Mater. Des.*, vol. 122, pp. 136–145, May 2017.

[52] G. Coroller *et al.*, “Effect of flax fibres individualisation on tensile failure of flax/epoxy unidirectional composite,” *Compos. Part A Appl. Sci. Manuf.*, vol. 51, pp. 62–70, Aug. 2013.

[53] X. Martinez, F. Rastellini, S. Oller, F. Flores, and E. Oñate, “Computationally optimized formulation for the simulation of composite materials and delamination failures,” *Compos. Part B Eng.*, vol. 42, no. 2, pp. 134–144, Mar. 2011.

[54] R. Joffe, J. Andersons, and L. Wallström, “Interfacial shear strength of flax fiber/thermoset polymers estimated by fiber fragmentation tests,” *J. Mater. Sci.*, vol. 40, no. 9–10, pp. 2721–2722, May 2005.

[55] A. Le Duigou, P. Davies, and C. Baley, “Exploring durability of interfaces in flax fibre/epoxy micro-composites,” *Compos. Part A Appl. Sci. Manuf.*, vol. 48, pp. 121–128, May 2013.

[56] A. Le Duigou *et al.*, “A multi-scale study of the interface between natural fibres and a biopolymer,” *Compos. Part A Appl. Sci. Manuf.*, vol. 65, pp. 161–168, Oct. 2014.